TECTONISM AND ENHANCED CRYOVOLCANIC POTENTIAL AROUND A LOADED SPUTNIK PLANITIA BASIN, PLUTO. P. J. McGovern[1], O. L White[2,3], and P. M. Schenk[1], [1]Lunar and Planetary Institute, USRA (3600 Bay Area Blvd., Houston, TX, 77058; mcgovern@lpi.usra.edu), [2]SETI Institute, Mountain View, CA, 94043, [3]NASA Ames Research Center, Moffett Field, CA, 94035.

Introduction: Pluto's near side hemisphere is dominated by Sputnik Planitia (SP), a vast, high albedo, glacial deposit composed of primarily N_2 ice that is filling an elongate impact basin reaching several km deep [1-4]. The uplands surrounding SP have been extensively tectonized [5,6]. Some tectonic lineations are oriented roughly radially or azimuthally to SP, and may potentially derive from the loading of the Sputnik basin with N_2 ice as well as the reorientation of Pluto in response to such loading [5], while the orientation of others suggest that they formed independently of Sputnik's influence [2,6]. Potential cryovolcanic features include the two imposing edifices to the south of SP, Wright and Piccard Montes [2,4], which reach >150 km across and >3.5 km tall, and display enormous central depressions that are tens of kilometers across and deeper than the edifices are tall. To the west of SP, accumulations of dark material are seen to mantle terrain surrounding Virgil Fossae in Cthulhu Macula [7] and fill portions of Uncama Fossae in Viking Terra [8]. These may represent ammoniated water ice deposits erupted as flows and fountains of cryoclastic materials from fissures along these troughs. The close spatial association of these putative cryovolcanic features with SP and surrounding tectonism is suggestive of a relationship based on enhancement of cryomagma ascent potential in an annular region beyond a large load on Pluto's H_2O ice shell/lithosphere [9]. Here we create detailed Finite Element Method (FEM) models of impact-driven lithospheric loading on Pluto and evaluate scenarios that are consistent with the spatial distribution of proposed cryovolcanic centers.

Modeling: We use the COMSOL Multiphysics FEM code to calculate models of the response of Pluto's icy shell lithosphere to infill of a Sputnik-sized impact basin (r = 400 km) by nitrogen ice. We use a flat-bottomed load profile to resemble observations of relatively "fresh" or "pristine" basins [e.g. 10] and the results of hydrocode impact models [e.g. 11,12]. The model also includes a "crustal collar" buoyant load at the base of the lithosphere, with Gaussian half-width 65 km and center at r_p = 600 km, reflecting crustal thickening expected from the impact process [11-13]. The shell (lithosphere) thickness is set to 50 km.

Fault type characterization. We characterize the faulting type predicted by the stress tensor within the shell using the Aψ parameter [14]. Values range over ±180°, with specific fault types corresponding to the labels above the brightest colors in Fig. 1b at values ±150° (thrust), ±90° (strike-slip) and ±30° (normal), with the sign determining the specific orientations of the faults, as labeled in Fig. 1.

Magma ascent criteria. We use 2 criteria for cryomagma ascent [15]: 1) The stress orientation criterion requires that the least compressive stress be oriented horizontally to allow vertical dikes to form. 2) We use the formulation of [16] to calculate the vertical gradient of tectonic stress (horizontal minus vertical normal stress), which when divided by planetary gravity gives an effective buoyant density $\Delta\rho_{efb}$ that can offset negative buoyancy of water in ice (about -80 kg/m^3).

Results: The applied basin-filling load produces compressional horizontal stress components σ_h and $\sigma\phi$ near the symmetry axis throughout most of the thickness of the lithosphere, grading from proximal generic compression to concentric thrust near the load edge. With increasing radial distance r_p, an extremely narrow zone of strike-slip is seen, followed by a broad zone of predicted faulting (failure criterion exceeded for 470 < r_p <900 km) consisting of proximal radial normal faulting and distal strike-slip mode distally.

For r_p > 450 km, a strike-slip regime is seen at the bottom and through most of the depth of the lithosphere, and for r_p > 700 km the entire lithosphere is in strike-slip mode. These findings stem from the extensional out-of-plane stress $\sigma\phi$ produced by the membrane response of a curved (spherical) lithosphere.[17]. The superposition of central downward load and outer buoyant also contributes to the observed relations.

The effective buoyant density calculated from the vertical gradient of the out-of-plane tectonic stress shows a region ranging from ≈ 420-680 km where $\Delta\rho_{efb}$ is greater than 80 kg/m^3, thereby allowing cryomagma ascent despite the negative buoyancy of water in ice. This region also satisfies the stress orientation criterion ($\sigma\phi$ > 0) throughout its entirety, again owing to the extensional membrane component of stress.

Discussion:

Tectonics. The model predicts extensional faulting (failure criterion exceeded) in radial geometry at the surface beyond the load from at r_p ≈ 470 km to 700 km. Several tectonic systems to the east and west of SP [6] exhibit sub-radial to radial orientations at these distances from the SP center. Yet further out, the strikes of some of these trends become oblique to a radial-concentric grid centered on SP, consistent with

potential strike-slip deformation at rp > 700 km in the model.

Cryomagmatism. The proposed sites of cryomagmatism (Wright and Piccard Montes, Virgil and Uncama Fossae) occur at distances 959, 1248, 914, and 612 km respectively from the center of SP's cellular region, where the N_2 ice is interpreted to be thickest (25°N, 175°E). In the cases of the Montes, these distances are significantly greater than the r_p values of the modeled zone of enhanced magma ascent (Fig. 1). However, the Montes are closer to the south-southeast extension of SP, a zone of loading that might become a significant or even primary influence that region, suggesting the need for further non-axisymmetric models. On the other hand, Uncama Fossae lies within the range of enhanced cryovolcanism shown in Fig. 1. Virgil Fossae is significantly beyond this range, but it lies on a radially-oriented system of fractures suggesting that it could be connected down-strike to the enhanced zone.

References: [1] Stern S.A. et al. (2015) *Science*, *350*, aad1815. [2] Schenk P.M. et al. (2018) *Icarus*, *314*, 400-433. [3] Umurhan O.M. et al. (2017) *Icarus*, *287*, 301-319. [4] Moore J.M. et al. (2016) *Science*, *351*, aad7055. [5] Keane J.T. et al. (2016) *Nature*, *540*, 90-93. [6] McGovern P.J. et al. (2019) *Pluto System After New Horizons*, Abstract #7063. [7] Cruikshank D.P. et al. (2019) *Icarus*, *330*, 155-168. [8] Cruikshank D.P. et al. (2020) *Icarus*, submitted. [9] McGovern P.J. and White O.L. (2018) *Cryovolcanism in the Solar System*, Abstract #2029. [10] Potter R.W.K. et al. (2013) *JGR Planets*, *118*, 963-979. [11] Potter R.W.K. et al. (2012) *GRL, 39* (18). [12] Johnson B.C. et al. (2016) *GRL*, *43*, 10,068-10,077. [13] Melosh H.J. et al. (2013), *Science, 340*, 1552-1555. [14] Simpson R.W (1997) *JGR Solid Earth*, *102*, 17,909-17,919. [15] McGovern P.J. & White O.L. (2019) *LPSC L,* Abstract #2994. [16] Rubin A.M. (1995) *Annu. Rev. Earth Planet. Sci., 23*, 287. [17] Turcotte D.L. et al. (1981) *JGR, 86*, 3951-3959. [18] Freed A.M. et al. (2001) *JGR Planets*, *106*, 20,603-20,620.

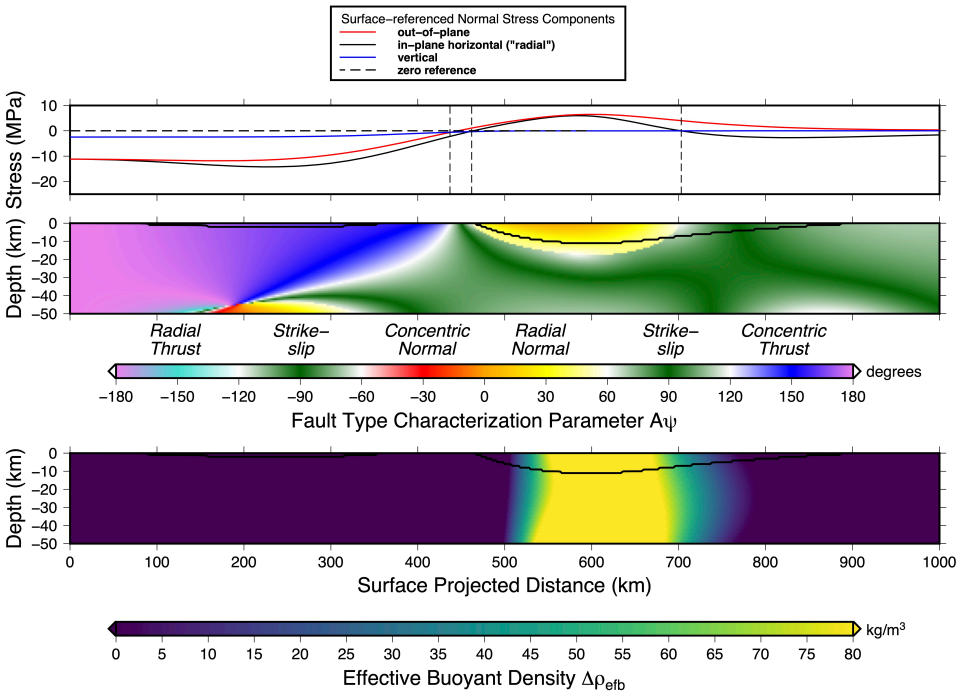

Figure 1. State of stress in an FEM model of Pluto's icy shell lithosphere, subject to loading by nitrogen ice infill of a Sputnik Planitia-sized basin. Horizontal coordinate r_p corresponds to distance from the symmetry axis at the surface of the spherical shell (after [18]). (A) Normal stress tensor components $\sigma\phi$ (out of plane, red curve) σ_h (horizontal in-plane, black curve) and σ_v (vertical, blue line) at the surface ($z = 0$) as functions of radius r_p from model center. Vertical dashed lines delineate major crossovers in normal stress magnitudes, corresponding to boundaries of predicted fault regimes in (B). (B) Cross-section map of the parameter $A\psi$ [14]. Color scale at bottom after [18], modified to give transitional colors between the regimes. "Pure" fault regime labels (corresponding to values of ± 30°, 90°, and 150°) are given atop color scale. Solid black contours bound regions where a Mohr-Coluomb failure criterion is satisfied. (C) Effective buoyant density $\Delta\rho_{efb}$ calculated from vertical gradient of the out-of-plane tectonic stress. Solid black contours as in (B).